
PERGAMON

Journal of the Mechanics and Physics of Solids
49 (2001) 1925–1935

JOURNAL OF THE
MECHANICS AND
PHYSICS OF SOLIDS

www.elsevier.com/locate/jmps

Influence of strain on functional characteristics of nanoelectronic devices

L.B. Freund[a,*], H.T. Johnson[b]

[a] *Division of Engineering, Brown University, Box D, 182 Hope Street, Providence, RI 02912-9104, USA*
[b] *Department of Aerospace & Mechanical Engineering, Boston University, Boston, MA 02215 USA*

Abstract

Charge transport through the crystal lattice of a nanoelectronic device occurs quantum mechanically. Incompatible elastic strain introduced during fabrication of a device modifies the lattice and, therefore, its functional characteristics can be affected. In this article, a computational model for assessing this influence is described. Consequences of strain which are expected to be significant for model development are identified and the modifications necessary in the Schrodinger equation, the governing equation for transport, to account for strain are indicated. The densities of confined electronic states which arise in a particular columnar SiGe device configuration are determined for a range of column diameters by means of the numerical finite element method, providing a quantitative illustration of the influence of strain on device characteristics.

Keywords: B. Semiconductor material; Thin films; C. Finite elements

1. Introduction

While the function of microelectronic devices—the control and manipulation of electric charge—is nonmechanical, stress introduced during fabrication can play a significant role both in the fabrication process itself and in the eventual electronic function of a device. The focus here is on the second of these issues. The purpose is to outline a modeling strategy which is being developed for quantitative assessment of the influence of mechanical strain on the functional characteristics of nanoelectronic devices.

The point of making semiconductor heterostructures is to exploit band edge offsets for confinement of electrons or holes. In this process of *band engineering*, epitaxial

* Corresponding author. Tel.: +1-401-863-1476; fax: +1-401-863-2857.
E-mail address: freund@engin.brown.edu (L.B. Freund).

0022-5096/01/$ - see front matter
PII: S0022-5096(01)00039-4

strain becomes a design parameter due to its influence on band edge energies. The role of uniform elastic strain from this point to view is reviewed by O'Reilly (1989) and by Yu et al. (1992).

The prefix *nano* is ubiquitous in the engineering and scientific literature nowadays, but its meaning is often vague. In the case of electronics, it is usually understood to imply that the mean-free-path of charge carriers between scattering sites is large compared to device dimensions. In such a case, charge transport is wave-like and is therefore appropriately described within the framework of quantum mechanics (Weisbuch and Vinter, 1991; Ferry and Goodnick, 1997). Thus, device modeling cannot be approached simply by extrapolating existing methodologies developed for diffusive transport in conventional devices.

The potential benefits to be realized from development of nanoelectronics are enormous. The efficiency of a microelectronic processor or memory chip is enhanced by increasing device density on the chip, by decreasing power consumption per device, or by reducing device response time. Order of magnitude improvements in each of these aspects are within reach. From a purely scientific point view, measurement of electronic transport characteristics is a means of spectroscopic interrogation of the electronic structure of the material, and quantitative modeling is required for interpretation of such experiments. Reliable models of transport processes in nanoelectronic devices which relate the material, processing and configurational features to functional characteristics of real devices are required to serve both the engineering and scientific objectives.

The motion of a carrier which is confined to a quantum well, a quantum wire or a quantum dot by surfaces or interfaces is *unrestricted* in two, one and zero space dimensions, respectively; these confining structures are collectively known as low-dimensional systems. The influence of nonuniform strain fields on band alignments and carrier confinement in low-dimensional systems was studied by Yang et al. (1997). They computed nonuniform strain fields in several heterostructures by means of the finite element method, and deduced band edge energy shifts on the basis of deformation potential. In recent work, the formulation introduced by Luttinger and Kohn (1955) for considering quantum mechanical fields which vary slowly on the atomic scale has been adopted as a basis for numerical solution of the steady-state Schrodinger equation in the presence of strain-modified potential fields, thereby extracting information about functional characteristics of strained heterostructures (Johnson et al., 1998; Johnson and Freund, 2001).

2. A device configuration

All types of nanoelectronic devices which achieve confinement without use of electric fields rely on a configuration with a small material volume of one semiconductor material (a quantum dot or quantum wire) embedded within another semiconductor material, forming a *semiconductor heterostructure*. With proper selection of materials, the interfaces provide barriers which confine charge. Perhaps the simplest exploitation of quantum effects in this way is the *resonant tunneling diode*, depicted schematically in Fig. 1. It consists of a potential well of a few nanometers width between two insulating

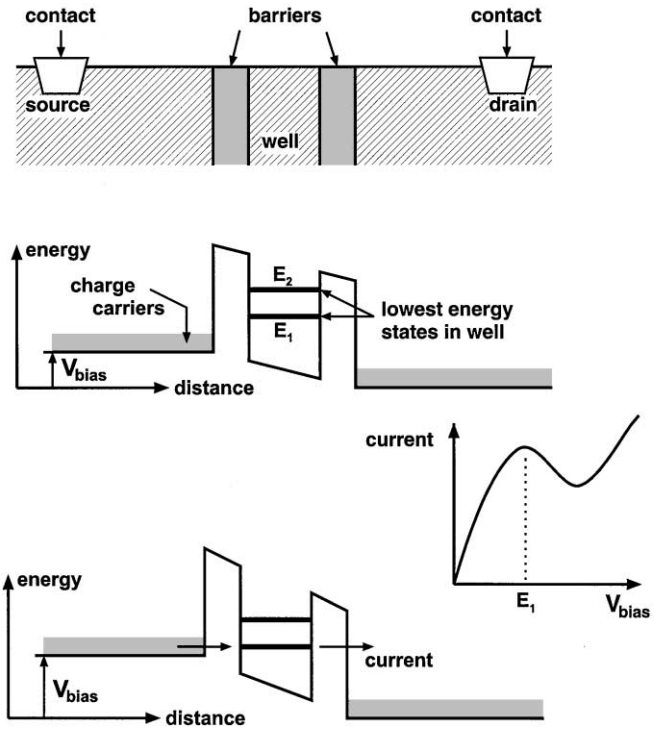

Fig. 1. Schematic diagram of a resonant tunneling device with two confined state energies. Note that peaks in current–voltage response correspond to energies of confined states.

barriers of similar width. If a charge carrier is confined in the well, quantum properties restrict its energies to one of a finite number of relatively high levels. If there is to be a current flow, the only way for carriers which are not sufficiently energetic to bypass the barriers is for the carriers to tunnel through the barriers. An imposed bias voltage on the device can elevate the energies of the available carriers to match the energy of the lowest confined state. In this state quantum mechanical tunneling, an energy conserving process, becomes possible. If the bias is further increased so that it falls between the confined state energy levels of the well, this energy correspondence is lost and the current falls. This behavior results in a dependence of current on bias voltage with peaks defined by the energies of confined states within the well. The connection between resonant peaks and energies of confined states is exploited in the modeling strategy which follows.

3. Strained heterostructures

Efforts to fabricate semiconductor heterostructures for quantum device applications have given rise to a wealth of interesting and important research issues in mechan-

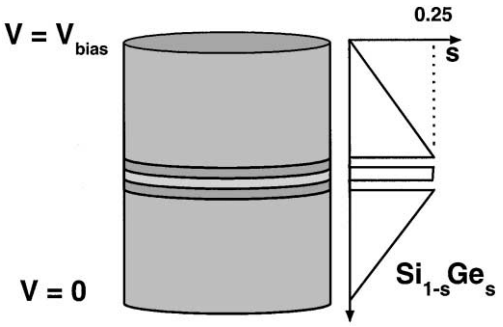

Fig. 2. A columnar semiconductor heterostructure with a SiGe quantum well layer between Si barrier layers, and with SiGe source and drain regions with gradation in Ge content. Device diameter is typically submicrum and layer thicknesses are a few nanometers.

ics (Freund, 1999), but such matters are outside the scope of the present discussion. Here, it is only noted that such configurations have certain common features which are important to take into account when developing quantitative models. For one thing, the material structures of interest must be free of extended defects. This condition is dictated by the requirement of functional uniformity among devices. The joined materials are typically of the same crystal class, say diamond cubic or zinc blende, and of the same crystallographic orientation. Materials are selected primarily on the basis of their electronic properties, and use of material combinations for which the stress free lattice parameters differ by as much as a few percent is common. In such cases, the kinematic constraint of epitaxy across the interface results in a residual elastic strain field which scales in magnitude with the lattice mismatch. Furthermore, due to the geometrical configurations necessary for confinement, the strain fields are spatially nonuniform. Because the electronic characteristics of a material depend on the lattice geometry, the nonuniformity in strain results in spatially nonuniform electronic characteristics.

To illustrate the degree of strain nonuniformity which can arise, consider the case of the columnar resonant tunneling diode illustrated in Fig. 2. Suppose that the well is a $Si_{1-s}Ge_s$ alloy where s is the atomic fraction of Ge, the barrier layers are Si, and the Ge content in the alloy is linearly diminished with distance from the barrier on each side. The lattice mismatch between $Si_{1-s}Ge_s$ and Si is $0.042s$. Suppose that the device is formed lithographically from a large area layered film grown on a Si substrate with a spatially uniform elastic strain. Upon creation of the lateral stress-free face of the column, however, the elastic strain is altered significantly, becoming relaxed in some portions of the column and increased in other portions. The variation of radial strain $\varepsilon_{rr}(r)$ with radial distance along the well midplane as computed by means of the finite element method is illustrated in Fig. 3 for several device diameters, illustrating the two main features of relaxation: one feature is confined to the vicinity of the free surface for all diameters and is controlled by the layer thickness; the other dominates away from the free surface and is controlled by the overall device dimensions.

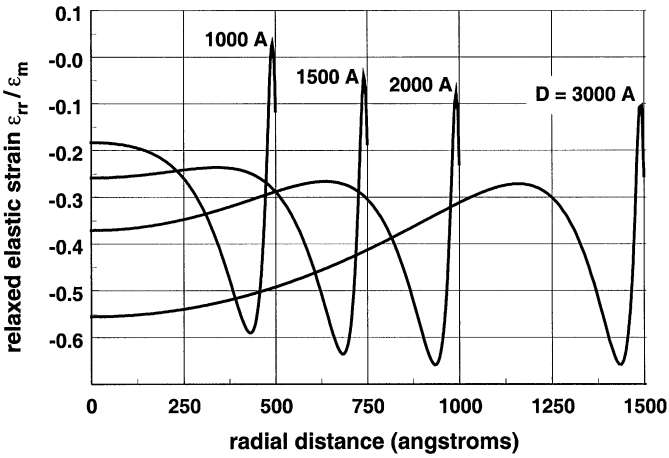

Fig. 3. Radial strain ε_{rr} versus distance along a radial line on the midplane of the quantum well. The strain arises from the fabrication process and is a consequence of the constraint of epitaxy enforced on the material interfaces.

4. Modification of the Schrodinger equation

The partial differential equation which governs the wave function $\Psi(\boldsymbol{x},t)$ is the Schrodinger equation,

$$-\frac{\hbar^2}{2m_0}\frac{\partial^2\Psi}{\partial x_j\partial x_j}(\boldsymbol{x},t)+V(\boldsymbol{x})\Psi(\boldsymbol{x},t)=-\mathrm{i}\hbar\frac{\partial\Psi}{\partial t}(\boldsymbol{x},t), \tag{1}$$

where $\hbar$ is Planck's constant, m_0 is the carrier mass which is equal in magnitude to the electron mass for transport of either holes or electrons, and $V(\boldsymbol{x})$ is a potential field through which the carrier must propagate. Principal contributions to $V(\boldsymbol{x})$ include the effects of the nuclei at lattice sites in the semiconductor crystal and the externally applied voltage, if any. Other factors affecting the potential field are variations in material properties from point-to-point in the structure and lattice distorting elastic strain. Only a single, isolated carrier is considered in this discussion. However, if multiple carriers were involved in transport, then their motions would be coupled through the contribution each carrier makes to the potential field of the others. The problem is one which involves multiple size scales, ranging from the spacing of the lattice to the overall scale of the device. If all geometrical dimensions of the heterostructure are large compared to atomic spacing and if all fields vary slowly on the scale of lattice spacing, then the discrete character of the lattice can be suppressed and can be taken into account in an approximate way.

Suppose that the Schrodinger equation is considered for the case when the only contribution to $V(\boldsymbol{x})$ in an unrestrained crystal is the contribution due to lattice interaction potential energy which has the periodicity of the crystal lattice. Assume a solution of the form

$$\Psi(\boldsymbol{x},t)=A(\boldsymbol{x})\mathrm{e}^{\mathrm{i}(\boldsymbol{k}\cdot x-E(\boldsymbol{k})t/\hbar)}, \tag{2}$$

where $E(\boldsymbol{k})$ is the conserved energy of the carrier wave at wave number $\boldsymbol{k}$. According to Bloch's theorem, the amplitude $A(\boldsymbol{x})$ is then also periodic with the period of the lattice. For any given $\boldsymbol{k}$, nontrivial solutions for $A(\boldsymbol{x})$ exist only for certain values of energy E, and the graphical representation of the resulting dependence of these admissible energies on wave number defines the *band structure* of the unstrained crystal. Accurate determination of band structure requires extensive computation for realistic interaction potentials of crystals; for some semiconductor materials, potentials which are able to represent all important aspects of material behavior are not yet available. The search for such potentials and their implications for band structure is the domain of basic semiconductor physics. The point of departure here, with a view toward learning about device performance, is in adopting useful descriptions of band structure which have reached some level of acceptance.

Charge transport in SiGe occurs by motion of holes, and the aspect of the band structure of most importance is that in the valence band adjacent to the semiconductor band gap. The valence band is comprised of a multitude of sub-bands, each representing a discrete admissible energy level at any particular value of $\boldsymbol{k}$, and a number of these sub-bands merge at the valence band edge, implying a degree of degeneracy. Most importantly for present purposes, the location of the valence band edge in wave number space coincides with the origin in that space, the so-called Γ point. It is precisely the small amplitude wave numbers in the vicinity of the Γ point which are presumed to dominate the wave motion representing transport. At the Γ point, the dependence of $E(\boldsymbol{k})$ on $\boldsymbol{k}$ is stationary under small changes in wave number, so a possible local representation of sub-band structure is

$$E = E_0 + \frac{\hbar^2}{2m_0}\boldsymbol{k}\cdot\boldsymbol{L}k, \tag{3}$$

where E_0 is the energy at the band edge with respect to some reference level and $\boldsymbol{L}$ is a second rank tensor representing the curvature of the dependence of E on $\boldsymbol{k}$ in the $\boldsymbol{k}$ direction; the factor $\hbar^2/2m_0$ appears only for the convenience of rendering the components of $\boldsymbol{L}$ dimensionless. A common simplifying assumption is that local behavior is isotropic, that is, $\boldsymbol{L} = L\boldsymbol{I}$ where $\boldsymbol{I}$ is the identity tensor, so that

$$E = E_0 + \frac{\hbar^2 L}{2m_0}\boldsymbol{k}\cdot\boldsymbol{k}. \tag{4}$$

This representation requires only two parameters, E_0 and L, for each sub-band.

It is well known that there is an unambiguous correspondence between dispersion relations and wave equations, in general. In the present instance, the dispersion relation in Eq. (4) is equivalent to the partial differential equation

$$-\frac{\hbar^2 L}{2m_0}\frac{\partial^2\Psi}{\partial x_j\partial x_j} + E_0\Psi = -\mathrm{i}\hbar\frac{\partial\Psi}{\partial t}, \tag{5}$$

the solution of which is valid in the region of validity of Eq. (4). The carrier mass m_0 is effectively replaced by $m_e = m_0/L$, the *effective mass*, and the lattice potential is replaced by the reference level E_0. Thus, for long wavelength behavior, the effect of the lattice is represented by the two parameters m_e and E_0. The former represents an alteration in inertial characteristics of a carrier due to the lattice, while the latter

represents a dielectric screening of a carrier from imposed fields due to the lattice. As a result, the device behavior can be pursued on the basis of the continuum wave equation

$$-\frac{\hbar^2}{2m_e}\frac{\partial^2\psi}{\partial x_j\partial x_j}(\boldsymbol{x})+V(\boldsymbol{x})\psi(\boldsymbol{x})=(E-E_0)\psi(\boldsymbol{x}), \tag{6}$$

where Eq. (6) no longer includes any influence of lattice spacing. For analysis of single sub-band behavior, E_0 is commonly set equal to zero and both E and $V(\boldsymbol{x})$ are referred to this same reference level. A subtle point is that the velocity which appears in Eq. (4) is the *group velocity* of the dispersive wave. As a consequence, the partial differential equation (6) governs the envelope function or Bloch function of the transport wave.

Strain enters the picture once it is recognized that band structure is determined from an interatomic potential expressed in terms of relative positions of the interacting nuclei in the periodic lattice. Although lattice spacing and orientation are not made explicit in Eq. (4), for example, the values of E_0 and L depend on geometrical details of the lattice. The lattice geometry for a cubic material, for example, can be specified in terms of three lattice vectors having specific orientation and magnitude. Starting from any lattice site, a relative position vector composed of a linear combination of any integer multiples of these lattice vectors locates another lattice site.

Let $\boldsymbol{a}$ denote a representative lattice vector and regard E_0 and L in Eq. (4) as functions of $\boldsymbol{a}$. If the ideal crystal is strained homogeneously then the lattice vectors deform into a set of new lattice vectors. Consider an arbitrary strain tensor $\boldsymbol{\varepsilon}$ which is small in magnitude and, without loss of generality, that strain occurs without rotation. The deformed lattice vector $\boldsymbol{a}'$ can then be expressed in terms of the undeformed counterpart as $\boldsymbol{a}'=\boldsymbol{a}+\boldsymbol{\varepsilon a}$. For any particular sub-band, the value of admissible energy at a given value of $\boldsymbol{k}$ is

$$E'(\boldsymbol{k})=E(\boldsymbol{k})+\frac{\partial E}{\partial \boldsymbol{a}}(\boldsymbol{k})\cdot(\boldsymbol{\varepsilon a}) \tag{7}$$

to first order in strain. This point of view makes it possible to represent the sensitivity of the sub-band features to strain in terms of sensitivity of the unstrained sub-band features to changes in lattice vectors. In particular, $V'=V+D_{ij}\varepsilon_{ij}$ and $L'=L+M_{ij}\varepsilon_{ij}$ where

$$D_{ij}=\frac{1}{2}\left[\frac{\partial E_0}{\partial a_i}a_j+\frac{\partial E_0}{\partial a_j}a_i\right],\quad M_{ij}=\frac{1}{2}\left[\frac{\partial L}{\partial a_i}a_j+\frac{\partial L}{\partial a_j}a_i\right]. \tag{8}$$

In reality, the value of D_{ij} is the sum of the contributions due to all lattice vectors, and similarly for M_{ij}. Although the strain-induced adjustments to effective mass and potential are determined on the basis of homogeneous deformation of the crystal, the result is applied pointwise for spatially varying strain throughout the device. The rationale for doing so is that strain is assumed to vary slowly on the scale of lattice spacing. Only the influence of strain on potential V is considered in the present study.

5. Computational approach

The general procedure for quantitative determination of the density of confined electronic states in the device of interest is as follows. First, for a heteroepitaxial device of given configuration and composition, the strain field induced by fabrication is determined, usually by means of finite element simulation of the process. With the strain field in hand and with knowledge of the electronic properties of the constituent materials in the absence of strain, the spatial distribution of effective mass (represented by the parameter L) and the carrier potential V are known. The form of the Schrodinger equation which governs the wave function $\psi(\boldsymbol{x})$ for a single sub-band is then

$$-\frac{\hbar^2}{2m_0}\frac{\partial}{\partial x_i}L(\vec{x})\frac{\partial\psi}{\partial x_i}(\vec{x}) + V(\vec{x})\psi(\vec{x}) = E\psi(\vec{x}), \tag{9}$$

where it has been anticipated that L may depend on position. The boundary and continuity conditions to be satisfied by the wave function are that $\psi = 0$ everywhere on the external boundary and that $Ln_i\partial\psi/\partial x_i$ must be continuous across any internal interface with unit normal vector n_i. A solution of this partial differential equation renders the functional

$$\Phi[\psi] = \int_R \left[-\frac{\hbar^2}{2m_0}\frac{\partial\bar{\psi}}{\partial x_i}L\frac{\partial\psi}{\partial x_i} + \bar{\psi}V\psi - \bar{\psi}E\psi\right] \mathrm{d}R, \tag{10}$$

stationary under variations in wave function $\delta\psi$ which vanish on the material boundary. Therefore, the variational requirement that $\delta\Phi = 0$ under variations $\delta\psi$ provides a weak form of the Schrodinger equation which serves as the basis for finding approximate solutions of Eq. (9) by means of the numerical finite element method (Johnson and Freund, 2001). Solutions of Eq. (9) can be found only for certain values of energy E, say $E_1, E_2, \ldots$, but not all correspond to confined states. The final stage in the analysis is to identify those particular eigen-solutions $\psi(\boldsymbol{x})$ for which the level curves of $|\psi(\boldsymbol{x})|^2$ are confined to be within the quantum well. The density of confined states for the device, in the form of number of states per unit energy E, can then be compared to the measured current–voltage behavior of the device.

6. An application

Transport experiments have been carried out at Brown University (Akyuz et al., 1998) on resonant tunneling diodes of the kind shown schematically in Fig. 2. The devices studied had diameters in the range from 2 μm down to 0.15 μm. The current versus bias voltage data from the experiments showed resonant tunneling peaks of the kind anticipated in the qualitative argument given above in connection with Fig. 1. The amplitude of measured current at the given bias voltage is expected to vary roughly in proportion to the cross sectional area of the device. If the structure were truly one-dimensional, on the other hand, the values of bias voltage at which resonant peaks arise would not vary with device diameter. However, the data showed that the voltages at which the peaks occurred deviated systematically from their values for large area

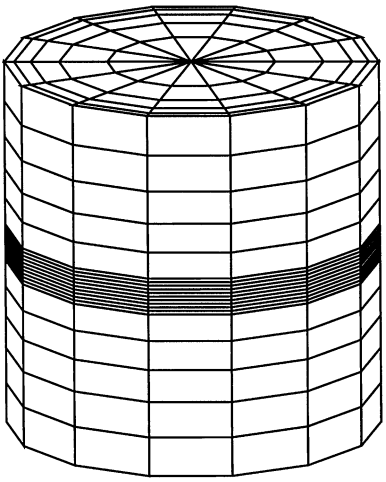

Fig. 4. A representative mesh used in a finite element simulation of the device shown schematically in Fig. 2. The same mesh is used to determine the elastic strain distribution, and subsequently to determine the wave functions of confined states.

devices, and it was hypothesized that this deviation is due to the influence of elastic strain. The lowest energy resonant peak, associated with transport of the so-called heavy holes, drifted toward larger energies as the diameter of the device was reduced, and a single sub-band of simulation was undertaken to examine the hypothesis. Assuming transport along the z or x_3 axis in the device, the heavy hole effective mass, represented by L in the Schrodinger equation in Eq. (9), is approximately $1/L = m_e = 0.537(1-s) + 0.284s$ for local Ge content s. The deformation potential matrix for heavy hole transport is given by

$$D_{ij} = \begin{bmatrix} a+b/2 & 0 & 0 \\ 0 & a+b/2 & 0 \\ 0 & 0 & a-b \end{bmatrix}, \tag{11}$$

where $a = 2.1(1-s) + 2.0s$ and $b = -1.5(1-s) - 2.2s$ in units of eV. The valence band offset of $Si_{1-s}Ge_s$ relative to Si is $0.56s$ eV. The strain and the valence band edge offset determine V in Eq. (9).

A representative finite element mesh is shown in Fig. 4. Node spacing is chosen to be smallest near the outer surface of the column and in the vicinity of the quantum well in order to capture the variation of fields in these critical portions of the structure.

All energy states confined to the quantum well were determined numerically by means of the finite element calculation. The result of the calculation is a discrete distribution of points on the energy axis, with one point for each confined state with due regard for any multiplicity of states at a given energy. To establish a continuous density of confined states plot, a narrow Gaussian distribution of unit amplitude was associated with each such point and all Gaussian curves were then added together. The

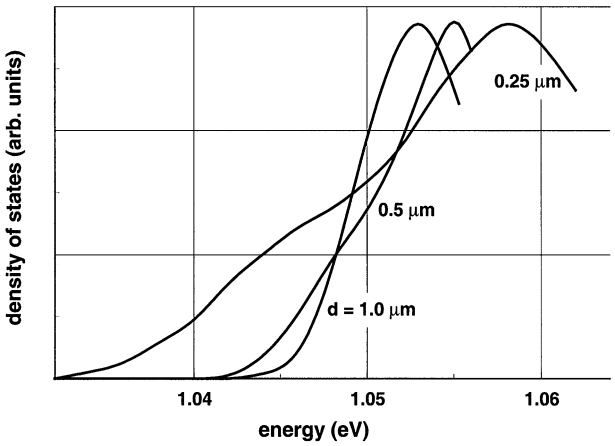

Fig. 5. Computed density of confined states for heavy hole transport in the device represented in Fig. 2 for three values of device diameter. The shift of the resonance peak toward higher energies with decrease in diameter is consistent with experimental observations.

result is a fairly smooth composite curve in arbitrary units versus confined state energy. The result of implementing this procedure for three different diameter devices is shown in Fig. 5 for diameters of 0.25, 0.5 and 1.0 μm. It is evident from these results that the energy at which the peak occurs for any given diameter drifts toward increasing values of energy as the device diameter is diminished, in a way which is consistent with the experimental observations.

7. A concluding note

Model development up to the present time, as reflected by the work outlined above, has focused largely on calculation of the density of confined electronic states of devices. Computational results for a particular resonant tunneling diode which has been characterized experimentally have been summarized and discussed on this basis. However, the density of states is not what is measured in characterizing any particular device. The long-term goal of work in this area is to produce synthetic current–voltage response characteristics for practical device configurations. More specifically, the idea is to understand the connections between the operational properties of a device and those physical features that can be produced reliably by means of existing fabrication process technology.

Acknowledgements

The research support at Brown University of the MRSEC Program of the National Science Foundation, under Award DMR-9632524, is gratefully acknowledged. The gen-

eral purpose finite element program *Abaqus* is licensed by Hibbitt, Karlsson & Sorensen Inc., Pawtucket, RI.

References

Akyuz, C.D., Zaslavsky, A., Freund, L.B., Syphers, D.A., Sedgwick, T.O., 1998. Inhomogeneous strain in individual quantum dots probed by transport measurements. Appl. Phys. Lett. 72, 1739–1741.

Ferry, D.K., Goodnick, S.M., 1997. Transport in Nanostructures. Cambridge University Press, New York.

Freund, L.B., 1999. The mechanics of electronic materials. Int. J. Solids Struct. 37, 185–196.

Johnson, H.T., Freund, L.B., 2001. The influence of strain on confined electronic states in semiconductor quantum structures. Int. J. Solids and Struct. 38, 1045–1062.

Johnson, H.T., Freund, L.B., Akyuz, C.D., Zaslavsky, A., 1998. Finite element analysis of strain effects on electronic and transport properties in quantum dots and wires. J. Appl. Phys. 84, 3714–3725.

Luttinger, J.M., Kohn, W., 1955. Motion of electrons and holes in perturbed periodic fields. Phys. Rev. 97, 869–883.

O'Reilly, E.P., 1989. Valence band engineering in strained-layer structures. Semicond. Sci. Technol. 4, 121–137.

Weisbuch, C., Vinter, B., 1991. Quantum Semiconductor Structures. Academic Press, San Diego.

Yang, M., Sturm, J.C., Prevost, J., 1997. Calculation of band alignments and quantum confinement effects in zero- and one-dimensional pseudomorphic structures. Phys. Rev. B 56, 1973–1980.

Yu, E.T., McCaldin, J.O., McGill, T.C., 1992. Band offsets in semiconductor heterostructures. Solid State Phys. 46, 1–146.